Enhanced alternative splicing of the *FLVCR1* gene in Diamond Blackfan anemia disrupts FLVCR1 expression and function that are critical for erythropoiesis

Michelle A. Rey,[1,2] Simon P. Duffy,[1,2] Jennifer K. Brown,[1,2] James A. Kennedy,[2,3] John E. Dick,[2,3] Yigal Dror,[1] and Chetankumar S. Tailor[1,2]

[1]Program in Cell Biology, The Hospital for Sick Children, Toronto, ON; [2]Department of Molecular Genetics, University of Toronto, Toronto, ON; [3]Division of Cell and Molecular Biology, University Health Network, Suite 8-355 Toronto Medical Discovery Tower, Toronto, ON, Canada

ABSTRACT

Background

Diamond-Blackfan anemia is a fatal congenital anemia characterized by a specific disruption in erythroid progenitor cell development. Approximately 25% of patients have mutations in the ribosomal protein RPS19 suggesting that Diamond-Blackfan anemia may be caused by a defect in ribosome biogenesis and translation. However, it is unclear how these defects specifically disrupt early erythropoiesis. Recent studies have shown that the retroviral receptor/heme exporter FLVCR1 is critical for early erythropoiesis. *FLVCR1* null mice, despite dying *in utero* and having reduced myeloid and lymphoid cell growth, show a disruption in early erythropoiesis and have craniofacial and limb deformities similar to those found in some Diamond-Blackfan anemia patients.

Design and Methods

In this study, we recapitulated the Diamond-Blackfan anemia hematologic features of reduced erythropoiesis but normal myelopoiesis by disrupting *FLVCR1* in human hematopoietic stem cells.

Results

We found that CD71^{high} cells, which are enriched for immature erythroid cells, from Diamond-Blackfan anemia patients negative for *RPS19* gene mutations express alternatively spliced isoforms of *FLVCR1* transcript which encode proteins whose expression and function are disrupted. More importantly, our results suggest alternative splicing of *FLVCR1* is significantly enhanced in Diamond-Blackfan anemia immature erythroid cells. Furthermore, we also observed enhanced *FLVCR1* alternative splicing and a dramatic reduction of FLVCR1 protein expression in RPS19 down-regulated human K562 cells, which were used as a model to represent *RPS19* gene mutated Diamond-Blackfan anemia.

Conclusions

Taken together, our results suggest enhanced alternative splicing of *FLVCR1* transcripts and subsequent FLVCR1 insufficiency as an additional contributing factor to the erythropoietic defect observed in Diamond-Blackfan anemia.

Key words: Diamond-Blackfan anemia, *FLVCR1*, retroviral receptor, heme exporter, alternative splicing.

Citation: Rey MA, Duffy SP, Brown JK, Kennedy JA, Dick JE, Dror Y, and Tailor CS. Enhanced alternative splicing of the FLVCR1 *gene in Diamond Blackfan anemia disrupts* FLVCR1 *expression and function that are critical for erythropoiesis. Haematologica 2008; 93:1617-1626. doi: 10.3324/haematol.13359*

Acknowledgments: we are grateful to James Ellis and Eyal Grunebaum for their critical reading of this manuscript. We are also grateful to Varun Charkravorty for his assistance in this study.

Funding: this work was supported by the Canadian Institutes of Health Research grant MOP-79541 and by the Sickkids Foundation grant XG07-028R.

Manuscript received May 15, 2008; Revised version arrived July 10, 2008; Manuscript accepted August 6, 2008.

Correspondence: Chetankumar S. Tailor, The Hospital for Sick Children, Program in Cell Biology, Room 7129 Elm Wing, 555 University Avenue, Toronto, ON, M5G 1X8, Canada.E-mail: chetankumar.tailor@sickkids.ca

Introduction

Diamond Blackfan anemia (DBA) is a rare inherited red blood cell disorder characterized by a moderate to severe reduction in the production of erythroid progenitor cells.[1–3] Current therapies such as steroids, blood transfusion, and bone marrow transplantation often have severe side effects or are ineffective in many DBA patients.[1,4-8] Approximately 40% of DBA patients have additional abnormalities that include short stature, cranofacial and urogenital malformations, heart defects and mental retardation.[1,8] DBA patients are also predisposed to develop acute myeloid leukemia, lymphoma and solid tumors.[5,8-10]

Approximately 25% of DBA patients have mutations in the gene encoding the S19 ribosomal protein (RPS19),[11,12] which is one of 33 ribosomal proteins that make up the 40S ribosomal subunit that is involved in translation.[13] Down-regulation of RPS19 in CD34$^+$ human hematopoietic stem cells disrupts erythroid progenitor cell but not myeloid cell development,[14,15] which mimics the hematologic features observed in DBA. Transfer of the *RPS19* gene into RPS19-deficient DBA bone marrow cells increases the number of erythroid progenitor cells,[16] which clearly demonstrates the importance of RPS19 in erythropoiesis. However, establishment of an RPS19 mouse model has proven difficult. Mice homozygous for the disruption of *RPS19* die *in utero* whereas mice heterozygous for *RPS19* alleles are normal with normal growth of all hematopoietic stem cells.[17] Recent studies have identified mutations in two additional genes encoding RPS24 and RPS17 in, respectively, 2% and 4% of RPS19-negative DBA individuals.[18,19] These findings suggest that DBA may be caused by a disruption in ribosome biogenesis and impairment in translation.[20] However, it remains unclear how these defects specifically disrupt early erythropoiesis.

Interestingly, the hematologic features of DBA show a striking similarity to the feline pure red cell aplasia found in domestic cats infected with the subgroup C feline leukemia virus (FeLV-C).[21-23] The feline anemia has been suggested to be caused by the FeLV-C envelope (Env) protein disrupting the cellular function of the heme exporter FLVCR1,[24] which is used as a receptor for entry by FeLV-C.[25-29] Disruption of FLVCR1 heme export function in human K562 erythroid cells induces apoptosis and disrupts K562 erythroid differentiation.[30] Furthermore, *FLVCR1* null mice, despite dying *in utero* and having reduced levels of myeloid and lymphoid cells,[31] show a severe disruption in the development of erythroid colony-forming units (CFU-E), and have the craniofacial and limb deformities found in some DBA patients.[1,8,31] These findings raise the possibility that DBA may be caused by a dysfunction in the human homolog of FLVCR1. Indeed, a previous linkage analysis identified four families with DBA exclusively linked to human chromosome 1q31,[24] the *FLVCR1* gene locus.[27] However, no genetic mutations were found in the exons of the *FLVCR1* gene.

In this study, we show that the hematologic features of DBA – disrupted early erythropoiesis but normal myelopoiesis – can be recapitulated *in vitro* in human hematopoietic stem cells by disrupting human FLVCR1 using FeLV-C Env protein. Moreover, we provide evidence of enhanced alternative splicing of *FLVCR1* transcripts, which disrupts the expression and function of FLVCR1 protein, in DBA immature erythroid cells negative for *RPS19* gene mutations, and in RPS19-reduced human K562 cells. We propose that enhanced alternative splicing of *FLVCR1* and FLVCR1 insufficiency contribute to the anemia seen in DBA.

Design and Methods

Bone marrow samples

Bone marrow aspirate samples were collected into preservative-free heparinized syringes. Marrow mononuclear cells were separated using Ficoll-Hypaque and cryopreserved as previously described.[32] Patients (D1-D5) were diagnosed with DBA based on published criteria,[33] which included chronic anemia, erythroid hypoplasia and either early onset (less than 1 year) or a first degree relative with DBA. No patient had evidence of severe aplastic anemia or malignant transformation at the time of collecting the bone marrow samples. Ten hematologically healthy normal (N1-N10) bone marrow donors served as controls. The studies were approved by the Institutional Research Ethics Board, and informed written consent was obtained from subjects or their legal guardians. An additional six bone marrow samples (N11-N16) were purchased from Stem Cell Technologies.

Cells and viruses

Phoenix-ampho cells (ATCC:SD3443) were cultured in high glucose DMEM (Invitrogen). FLYRD18,[34] TE671, TELCeB6,[34] HeLa and *Mus. dunni* tail fibroblast (MDTF) cells were cultured in low glucose DMEM (Invitrogen). Human K562 cells were cultured in IMDM medium (Invitrogen). All media were supplemented with 10% fetal bovine serum (FBS) (Invitrogen). FLYRD18, TELCeB6 and phoenix ampho cells are retroviral packaging cells, which were used for infection studies. β-galactosidase encoding FeLV-C and FeLV-B pseudotyped viruses were generated by transfection [SuperFect reagent (Qiagen)] of TELCeB6 cells with pFBCsalf[29] and pFBFGBsalf[35] retroviral expression vectors, respectively. Transfectants were selected with pheomycin (50 μg/mL), resistant colonies were pooled, and virus supernatant was used to infect target cells. Target cells were infected with β-galactosidase encoding FeLV-C and FeLV-B and infected cells were stained as previously described.[36]

Generation of retroviruses carrying FeLV-B or FeLV-C Env genes

FeLV-B and -C envelope (Env) cDNA were amplified by polymerase chain reaction (PCR) using the pFBCsalf and pFBFGBsalf vectors and the FeLV Env primers 5'-GGGGGGATCCATCAAGATGGAAAGTCCAACG-CACCCA-3' containing a BamHI restriction site, and 5'-GGGGCTCGAGTCATGGTCGGTCCGAATCG-TATTG-3' containing a XhoI restriction site. The amplified Env cDNA were cloned into the pFBneo retroviral expression vector (Stratagene, Cedar Creek, TX, USA).

Phoenix-ampho cells were transfected with the respective vector or Env expression constructs, and virus supernatant was used to infect FLYRD18 packaging cells. Transduced FLYRD18 cells were selected with G418 (1.0 mg/mL), resistant colonies pooled, and virus supernatant used to transduce target cells (see below). Virus titer was determined by incubating human HeLa cells with serial dilutions of virus for 4 hours with polybrene (8 μg/mL) (Sigma-Aldrich) followed by selection with G418 (1.0 mg/mL). Resistant colonies were stained with trypan-blue and counted.

Introduction of FeLV Env genes into human TE671 cells and human hematopoietic stem cells

TE671 cells were transduced with retroviruses isolated from Env and vector transduced FLYRD18 cells, selected with G418, and tested for susceptibility to β-galactosidase encoding FeLV-C and FeLV-B. Lineage-depleted (Lin-) umbilical cord blood cells[37] were also transduced with Env and vector-containing retroviruses after first concentrating the virus by ultracentrifugation (30,000 rpm) at 4°C for 90 min in a Beckman SW41Ti rotor, and resuspension in XVIVO-10 media (BioWhittaker, Walkersville, MD, USA). Erythroid cell growth of transduced Lin-cord blood cells was induced as previously described.[37] Transduced cells were analyzed after day 6, 10, 13 and 17 by flow cytometry using anti-CD36-FITC, anti-GlyA-PE, and anti-CD45-PCS antibodies. Myeloid cell growth was induced by incubation of cells in IMDM (StemCell Technologies) supplemented with 1.5 mg/mL G418, 15% FBS, interleukin-3 (2 ng/mL) and stem cell factor (20 ng/mL). Cell samples were analyzed by flow cytometry using anti-CD14-PE, anti-CD15-FITC.

RNA isolation from CD71^{high} cells

Bone marrow aspirates from normal and DBA patients were thawed in RPMI medium (Sigma) containing 10% fetal bovine serum (FCS) (Sigma) and 0.1 μg/mL DNAse (Sigma). Approximately 1×10^5 cells were washed twice in cold phosphate-buffered saline (PBS) containing 0.5% bovine serum albumin (BSA, Sigma), and stained with 20 μL anti-CD71-PE (BD Biosciences) conjugated antibody at 4°C for 1 hour in the dark. Cells were then washed twice to remove unbound antibody and sorted into CD71^{high} or CD71^{low} and CD71$^-$ cells using a fluorescence activated cell sorter (BecktonDickson). Total RNA was extracted from sorted cells using an RNeasy RNA preparation kit (Qiagen) and total cDNA was prepared using Thermoscript reverse transcriptase (Invitrogen).

Isolation of FLVCR1, Pit1 *and* EPOR *sequences from Diamond Blackfan anemia and normal erythroid cells*

FLVCR1 sequences were amplified by PCR using Expand Hi-Fidelity *Taq* DNA polymerase (Roche) using cDNA isolated from five DBA (D1-D5) and ten normal (N1-N10) cell samples (see above), and specific primers that primed to *FLVCR1* cDNA encoding the transmembrane (TM) 1 sequence (FLVCR1-TM1 primer: 5'-TACTCGCTGGTCAACGCCTTTCAGTGG-3') and TM12 sequence (FLVCR1-TM12 primer: 5'-TCTTCGCAGATCAGACTTGATTAATGCTGTTAA-3'). The PCR was run according to the manufacturer's protocol. Amplified products were cloned into pCR2.1TOPO vector (Invitrogen) and subsequently sequenced (ACGT Corporation, Toronto, Canada). Sequences encoding the Pit1 phosphate symporter and the erythropoietin receptor (EPOR) were also amplified by PCR using Pit1 primers (Pit1-F primer 5'-CCGC-CGCTTCTGGTCCTTTGGTGG-3'; Pit1-R primer 5'-CGCCAGTCAACAGCCTTCTTGGACC-3') and EPOR (EPOR-F primer 5'-ATGGACCACCTCGGG-GCGTCCCTCTGG-3'; EPOR-R primer 5'-CTAAGAG-CAAGCCACATAGCTGGG-3')

Construction of HA-tagged E3$^-$ and E3$^-$E6$^-$ retroviral expression constructs

cDNA encoding the N-terminal of *FLVCR1* was ligated to the E3$^-$ or E3$^-$E6$^-$ FLVCR1 cDNA by first digesting pFBneoFLVCR1HA,[36] containing the full-length *FLVCR1* cDNA with 3' HA tag, with the BamHI restriction enzyme, which removes the C terminal two-thirds of the *FLVCR1* sequence. The E3$^-$ or E3$^-$E6$^-$ FLVCR1 sequence, cloned in pCR2.1TOPO vector, was isolated by BamHI digestion and was subsequently cloned in the BamHI-digested pFBneoFLVCR1HA to generate, respectively, the E3$^-$-N and E3$^-$E6$^-$-N vectors. cDNA encoding the HA-tagged C-terminal sequence of *FLVCR1* was isolated from the pFBneoFLVCR1HA vector by digestion with AseI and was then ligated to an AseI-digested E3$^-$-N or E3$^-$E6$^-$-N vector to generate respectively, E3$^-$HA and E3$^-$E6$^-$HA FLVCR1. Phoenix-ampho cells were then transfected with the respective expression constructs, and virus supernatant from the transfected phoenix-ampho cells was used to introduce the HA-tagged E3$^-$ or E3$^-$E6$^-$ FLVCR1 cDNA into murine MDTF cells. Transduced MDTF cells were selected using G418 (1.5 mg/mL) and tested for susceptibility to lacZ virus infection.

Protein expression profile

Cellular expression of HA-tagged FLVCR1 proteins was analyzed by western blotting as previously described.[36] Cellular localization of the HA-tagged proteins in target cells was analyzed by immunofluorescence. Briefly, target cells were fixed with 2.5% paraformaldehyde and permeabilized with 0.05% Triton-X-100 in PBS, after overnight growth. Staining was performed with a 1:500 dilution of monoclonal anti-HA.11 antibody (Covance, QC, Canada) followed by incubation with a 1:500 diluted goat anti-mouse antibody conjugated to Cy3. Cell DNA was stained with 0.1 mg/mL DAPI DNA counter stain (Sigma). Fluorescence was visualized with a Zeiss LSM 510 Axiovert confocal microscope with 63X oil objective magnification.

Quantitative real-time PCR

Gene expression was quantified by Q-PCR using an ABI7900 real-time PCR machine with SYBR Green master mix (Applied Biosystems, CA, USA). Q-PCR was performed using total cDNA isolated from DBA and normal CD71^{high} cells and the following primers. Gene expression was calculated relative to actin B gene expression (ActB-F

primer: 5'-TGCGTGACATTAAGGAGAAG-3'; ActB-R primer: 5'-AGGAAGGAAGGCTGGAAGAG-3'). Total *FLVCR1* transcript expression was quantified using exon 1-specific primers (E1 primer: 5'-TCCATGGTGTACATGCTGGCCTA-3'; αE1 primer: 5'-AGGAGATGTTGTTGCACAGTGCCG-3'). E2 and E3 containing *FLVCR1* transcripts were quantified using the E2 primer 5'-GAACATCAGCTGTTGCCACA-3', and the αE3 primer 5'-TGTCTTGAAGAGCTGCTTGA-3'. To eliminate the possibility of genomic contamination, Q-PCR was also performed using *FLVCR1* intron 1-specific primers (intron1-F primer: 5'-AGTTCCTGGCACATAAGGGACACA-3'; intron1-R primer: 5'-GCCTCCCAAAGTGCTGAGATTACA-3'). *RPS19* gene expression was quantified using the RPS19-F primer 5'-AAAGACGTGAACCAGCAGGAGTTC-3', and the RPS19-R primer 5'-AGGAAGGAAGGCTGGAAGAG-3'.

RPS19 shRNA expression in human K562 cells

The RPS19 shRNA R1 and R2, and the Luciferase (Luc) shRNA retroviral constructs were kindly provided by Dr. Colin A. Sieff.[14] Phoenix ampho cells were transfected with the shRNA constructs, and virus supernatant was used to transduce human K562 cells. R1, R2 or Luc transduced cells were selected using puromycin (1.0 mg/mL) and resistant cells were pooled. Transduced K562 cells were subsequently analyzed for RPS19 and FLVCR1 protein expression by western blotting using anti-RPS19 monoclonal antibody (Abnova Corporation, Taiwan) and anti-FLVCR1 polyclonal antibody, respectively (Abcam, Cambridge, MA, USA). *RPS19* and total *FLVCR1* transcript expression, and expression of E2 and E3 containing *FLVCR1* transcript was quantified as outlined above.

Results

Disruption of human FLVCR1 affects erythropoiesis but not myelopoiesis, which recapitulates the hematologic features of Diamond Blackfan anemia

To investigate a potential role for human FLVCR1 in DBA, we set up a cell culture system to investigate the effect of FLVCR1 disruption on human erythropoiesis and myelopoiesis. FLVCR1 function was disrupted by expression of the envelope (Env) protein from the subgroup C feline leukemia virus (FeLV-C). Previous studies showed that FeLV-C infection of target cells disrupts both subsequent FeLV-C virus infection[28,38] and FLVCR1 heme export,[30] which led to the hypothesis that the FeLV-C Env protein disrupts FLVCR1. To show that FeLV-C Env specifically disrupts human FLVCR1, we expressed FeLV-C Env in human TE671 cells. As shown in Figure 1, FeLV-C Env expression in human TE671 cells (TE671/C Env) specifically reduced subsequent FeLV-C infection but not infection of the related FeLV-B virus, which binds to and uses the human inorganic phosphate symporter Pit1 for entry.[39-41] FeLV-C Env expression reduced FeLV-C infection by approximately 50,000-fold when compared to infection of parental TE671 cells (Figure 1, TE671/C Env). Conversely, expression of FeLV-B Env in TE671 cells reduced subsequent FeLV-B infection by 20,000-fold but did not significantly affect FeLV-C infection. These findings show that FeLV-C Env specifically disrupts human FLVCR1. The reduction of virus infection was significant but partial thus suggesting that not all FLVCR1 molecules are blocked.

We next introduced the FeLV-B Env gene, FeLV-C Env gene or a control vector into lineage-depleted human umbilical cord blood cells by retroviral transduction, and cultured the cells for 13 days in a liquid culture system that promoted erythroid differentiation. Using flow cytometry, we quantified the percentage of transduced cells that expressed the glycophorin A (GlyA) cell surface protein, which is specifically expressed on mature erythroid cells such as early and late erythroblasts. As shown in Figure 2A, both vector- and FeLV-B Env-transduced cells exhibited an expression profile characteristic of normal erythroid development with approximately 39-43% of transduced cells being $GlyA^+$ by day 13 (Figure 2A, upper two quadrants). Interestingly, cells transduced with FeLV-C Env gene showed a marked delay in erythroid maturation, as approximately 20% of the transduced cells expressed GlyA (Figure 2A). Consistent with these findings, analysis of CD45 surface protein, which is normally down-regulated during erythroid maturation, showed that there were 56-65% fewer $CD45^-$ cells in the FeLV-C Env-transduced culture compared to the vector- and FeLV-B Env-transduced culture (Figure 2B, lower left quadrant). These findings suggest a major disruption in erythroid development in FeLV-C Env-transduced cultures.

To assess whether the effect of FeLV-C Env was specific to erythroid development, vector- FeLV-B Env or FeLV-C Env-transduced cells were also grown in myeloid growth medium. After 13 days of culture, specific myeloid cells were identified by flow cytometry using antibodies to CD14 (monocytes/macrophages) and CD15 (myelocytes/granulocytes) surface proteins. As shown in Figure 2C, we did not find significant differences in myeloid cell growth between vector- FeLV-B Env- and FeLV-C Env-transduced cells. We observed a similar specific disruption in erythropoeisis but not myelopoiesis in the FeLV-C Env-transduced culture in a repeated independent experiment (*data not shown*). We also assessed

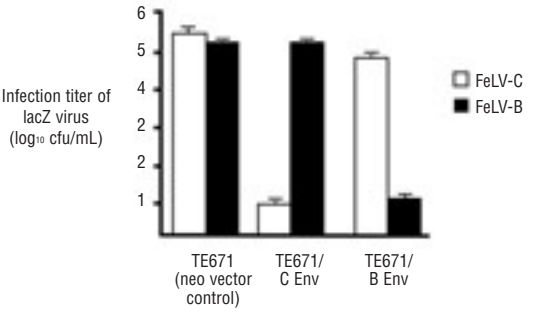

Figure 1. Susceptibility of human TE671 cells expressing FeLV-C or FeLV-B Env proteins to FeLV-C and FeLV-B infection. FeLV-C (C Env) or FeLV-BEnv (BEnv) genes were introduced into TE671 cells by retroviral infection, and infected cells were selected using G418. Transduced cells were then tested for susceptibility to infection by β-galactosidase encoding FeLV-C (white) and FeLV-B (black). Titers are the average of three experiments and are represented as colony-forming units (cfu) per milliliter of virus supernatant.

expression of FeLV Env proteins in the erythroid cultures. We found that expression of FeLV-B Env was higher in the erythroid cultures than expression of FeLV-C Env (*data not shown*). These findings suggest that Env expression level was not responsible for the disruption in erythropoiesis observed in the FeLV-C Env-transduced cultures. Taken together, our results suggest that FeLV-C Env expression specifically disrupts early erythropoiesis but not myelopoiesis, which recapitulates the hematologic features observed in DBA, and in cats infected with FeLV-C. Given that FeLV-C Env significantly but partially blocks human FLVCR1 (Figure 1), our results imply that a significant but partial block of human FLVCR1 can recapitulate the hematologic features of DBA, and supports a role for FLVCR1 in the pathogenesis of DBA.

Isolation of alternatively spliced FLVCR1 *isoforms from Diamond Blackfan anemia erythroid cells*

To further investigate a role for FLVCR1 in DBA, we analyzed *FLVCR1* sequences from immature erythroid cells isolated from five DBA (D1-D5), and ten normal (N1-N10) bone marrow samples. All DBA patients were identified as being negative for *RPS19* gene mutations. Samples from DBA patients positive for *RPS19* gene mutations were not available for this study. Using antibodies specific to CD71, we isolated a population of cells expressing high levels of the CD71 surface protein (CD71^{high}), which are enriched for immature erythroid cells.[15,42] Consistent with the low levels of erythroid progenitor cells in DBA patients,[1-3] we isolated fewer CD71^{high} cells from each of the five DBA samples than from the ten normal samples (*data not shown*). Using PCR and primers specific to FLVCR1 TM 1 and 12 (Figure 3, black arrows) coding regions, we amplified *FLVCR1* cDNA of approximately 1.2 kbp in size from DBA and normal CD71^{high} cells. We subsequently cloned the amplified cDNA in a PCR cloning vector and sequenced clones from each of the DBA samples D1-D5 and from each of the normal samples N1-N10. Interestingly, in addition to amplifying the expected 1.2 kbp *FLVCR1* cDNA, we also amplified cDNA of 1.0-1.1 kbp in size in each of the DBA and normal samples (*data not shown*). Subsequent sequencing showed that the 1.2 kbp sequence was *FLVCR1* with no mutations. Interestingly, the 1.0-1.1 kbp sequences were also *FLVCR1* but contained specific exon (E) sequence deletions. We isolated normal spliced *FLVCR1* and an E6$^-$ (exon 6 deleted) *FLVCR1* from all five DBA and ten normal samples (Figure 3). In addition, we isolated four alternatively spliced *FLVCR1* isoforms, E3$^-$, E3$^-$ E6$^-$, E2$^-$, and the E2$^-$

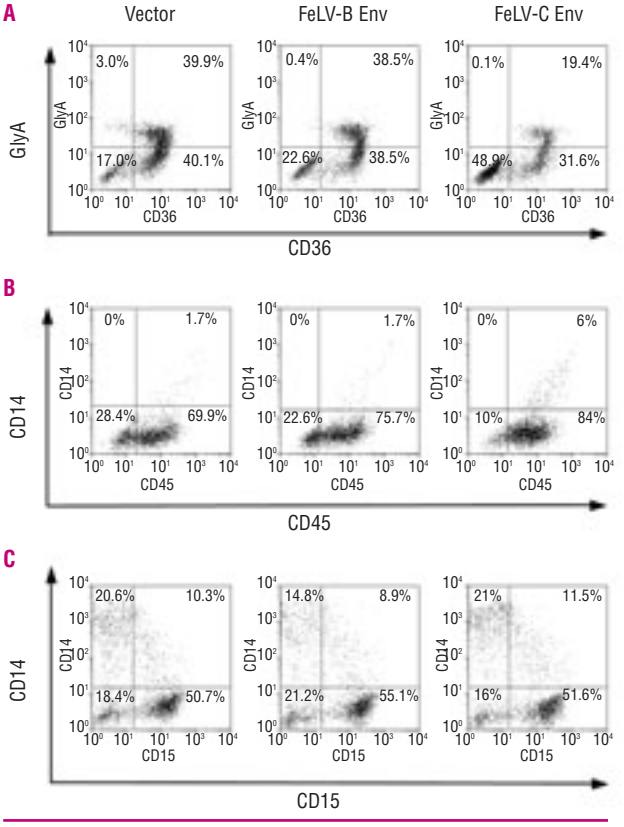

Figure 2. Erythroid and myeloid cell development of vector-, FeLV-B Env- or FeLV-C Env- transduced lineage-depleted cord blood cells. FeLV-C and FeLV-B Env genes were introduced into lineage depleted cord blood cells by retroviral infection and cells were subsequently cultured in either erythroid or myeloid growth medium. Surface expression of CD36, GlyA, CD14, CD15 and CD45 was analyzed by flow cytometry after 13 days of culture in the respective growth media. (A) CD36 and GlyA surface expression on vector- and FeLV Env-transduced cells grown in erythroid growth medium. The percentages of cells expressing GlyA are shown in the upper two quadrants. (B) CD14 and CD45 expression on FeLV Env- and vector- transduced cells grown in erythroid growth medium. CD45- cells are represented in the two left quadrants. (C) CD14 (monocyte/macrophage) and CD15 (myelocyte/granulocyte) expression on FeLV Env- and vector- transduced cells grown in myeloid growth medium. The percentages of cells expressing CD14 and CD15 markers are shown.

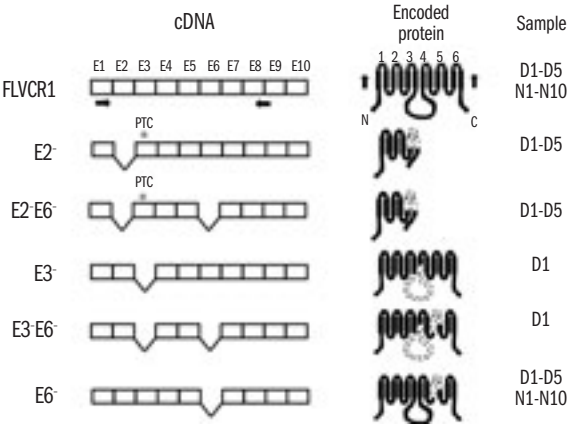

Figure 3. Alternatively spliced *FLVCR1* isoforms isolated from Diamond Blackfan anemia and normal immature erythroid cells. Alternatively spliced *FLVCR1* isoforms were isolated from five Diamond Blackfan anemia (D1-D5) and ten normal (N1-N10) samples by PCR using primers encoding FLVCR1 transmembrane (TM) 1 and 12 (black arrows). Amplified sequences were cloned into a PCR cloning vector and subsequently sequenced. *FLVCR1* exons (E) 1-10 are shown as boxes. *FLVCR1* sequences are labeled E2$^-$ (exon 2 deleted), E2$^-$E6$^-$ (exon 2 and 6 deleted), E3$^-$ (exon 3 deleted), E3$^-$E6$^-$ (exon 3 and 6 deleted) and E6- (exon 6 deleted). The premature termination codon is denoted by an asterisk. A diagram of the topology of potential proteins encoded by the alternatively spliced *FLVCR1* sequences is also shown. Normally spliced *FLVCR1* encodes a cell surface protein predicted to contain 12 transmembrane spanning segments with six presumptive extracellular loops (loop numbers are indicated above the loops). The Diamond Blackfan anemia and normal samples from which the *FLVCR1* sequences were isolated are also denoted.

E6⁻ from DBA samples but not from normal samples. Figure 3 also shows a diagram of the potential proteins encoded by the alternatively spliced *FLVCR1* isoforms. Splicing of *FLVCR1* E3 or E6 causes in-frame deletions that encode potential proteins with major deletions (Figure 3, hashed lines). Interestingly, splicing of E2 causes a frame-shift deletion, which results in the generation of a premature termination codon (Figure 3, see PTC) that potentially encodes a truncated protein. Together, these findings suggest that DBA CD71^{high} cells express alternatively spliced *FLVCR1* sequences that are not expressed, or weakly expressed (*see below*), in normal CD71^{high} cells.

To ascertain the specificity of the alternatively spliced *FLVCR1*, we amplified cDNA sequences encoding two additional human cell surface proteins. We amplified sequences encoding the FeLV-B receptor Pit1, and sequences encoding the erythropoietin receptor (EPOR),[43] which is a major protein expressed on the surface of erythroid cells. We isolated the expected cDNA of 1.6 kb and 2.0 kb, respectively, from each of the five DBA and ten normal erythroid cell samples. Subsequent sequencing of the amplified Pit1 and EPOR cDNA did not identify alternatively spliced isoforms of either Pit1 or EPOR. These results suggest, within the limitations of this study, that alternative splicing in DBA immature erythroid cells is unique to *FLVCR1*.

Alternatively spliced FLVCR1 *transcripts encode proteins that have disrupted cellular and surface expression, and receptor function*

We next characterized the expression profile and receptor function of the E3⁻ and E3⁻E6⁻ encoded proteins. As described above, splicing of E3 or E6 in *FLVCR1* transcripts causes an in-frame deletion that could potentially encode a functional protein. We expressed HA-tagged E3⁻, E3⁻E6⁻ or full-length *FLVCR1* cDNA in murine MDTF cells, and tested the susceptibility of these cells to FeLV-C infection. Consistent with our previous findings,[36] parental MDTF cells were resistant, whereas MDTF cells expressing full-length human FLVCR1 were highly susceptible, to FeLV-C infection (Figure 4A, control and hFLVCR1). Interestingly, we found that the E3⁻ and E3⁻E6⁻ transduced MDTF cells were weakly susceptible to FeLV-C. Infection titers were 100,000-500,000 fold less than titers on MDTF/hFLVCR1 cells (Figure 4A).

To investigate the relative resistance of E3⁻ and E3⁻E6⁻ *FLVCR1*-transduced murine cells to FeLV-C, we analyzed the cellular expression of the encoded proteins in cell lysate fractions. We found that the E3⁻ and E3⁻E6⁻ encoded proteins were weakly expressed compared to full-length FLVCR1 (Figure 4B). Using confocal microscopy, we further found that the E3⁻ and E3⁻E6⁻ encoded proteins were predominantly dispersed within the cell (Figure 4C). In contrast, full-length FLVCR1 was predominantly localized at the cell membrane (see white arrows in Figure 4C) consistent with FLVCR1 being a cell surface protein. Taken together, these findings suggest that the cellular and surface expression, and receptor function of E3⁻ and E3⁻E6⁻ encoded proteins are disrupted.

Alternative splicing of FLVCR1 *transcripts is enhanced in Diamond Blackfan anemia immature erythroid cells*

To investigate the significance of the alternatively spliced *FLVCR1* in DBA, we quantified the expression levels of alternatively spliced *FLVCR1* transcripts in DBA samples and compared these to the expression in normal samples. We used six new normal samples (N11-N16) enriched for CD71^{high} expressing cells in addition to samples N5, N7, N9 and N10. Samples N1-N4, N6 and N8 were not used because of insufficient sample material. Using total cDNA prepared from each DBA and normal sample, and using the E1/αE1 primers (Figure 5A, inset), we quantified, by real-time PCR, total *FLVCR1* (normal and alternatively spliced) transcript expression relative to actin B gene expression. We found that total *FLVCR1* transcript expression was significantly down-regulated in DBA samples D1-D5 compared to expression levels in the ten normal samples (Figure 5A). The exception was normal sample N15, which had a reduced level of *FLVCR1* transcript expression. We next used the E2/αE3 primers (Figure 5A, inset) to quantify expression levels of *FLVCR1* transcripts containing both

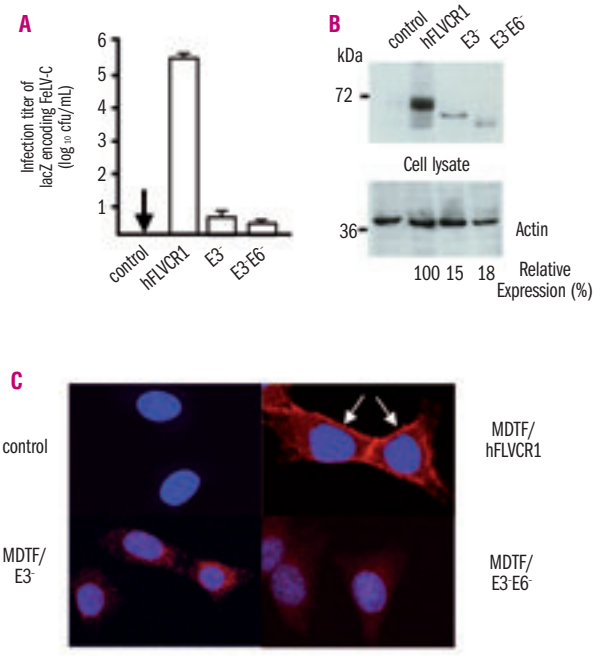

Figure 4. Expression and functional analysis of the E3⁻ and E3⁻E6⁻ *FLVCR1* encoded proteins. HA-tagged normal *FLVCR1*, and E3⁻ and E3⁻E6⁻ *FLVCR1* sequences were introduced into murine *Mus. dunni* tail fibroblast (MDTF) cells by retroviral infection. Cells were subsequently tested for susceptibility to β-galactosidase expressing FeLV-C, and E3⁻ and E3⁻E6⁻ FLVCR1 protein expression analyzed by western blotting and by confocal microscopy (A) Susceptibility of murine MDTF cells expressing human *FLVCR1*, E3⁻ or E3⁻E6⁻ encoded proteins to β-galactosidase expressing FeLV-C. Control represents parental MDTF cells. Infection titers are the averages of three experiments and are represented as colony-forming units (cfu) per milliliter of virus supernatant. The arrow indicates zero infection titer (B) Western blot analysis of HA-tagged E3⁻, E3⁻E6⁻, and hFLVCR1 proteins in cell lysate fractions from *FLVCR1*-transduced MDTF cells. (C) Confocal immunofluorescence microscope image of MDTF cells (control), and MDTF cells expressing HA-tagged human FLVCR1, E3⁻ or E3⁻E6⁻ FLVCR1. The white arrows depict surface localization. The nucleus of the cell is stained with DAPI.

E2 and E3, and calculated the percent of E2/E3-containing *FLVCR1* transcripts relative to total *FLVCR1* transcripts. As shown in Figure 5B, we found that approximately 5-45% of *FLVCR1* transcripts in the DBA samples contained both E2 and E3 compared to 76-96% E2/E3-containing transcripts in the normal samples. These findings clearly suggest a significant disruption in FLVCR1 E2 and E3 in the DBA samples, and imply a dramatic enhancement in alternatively spliced *FLVCR1* transcripts in the DBA samples compared to in the normal samples.

Down-regulation of RPS19 enhances alternative splicing of FLVCR1

To ascertain whether alternative splicing of *FLVCR1* is enhanced in DBA containing *RPS19* gene mutations, we used human K562 cells down-regulated in RPS19 as a model. Previous studies have used RPS19 down-regulated human cells as a model system to represent *RPS19* mutated DBA.[14,15] We independently expressed two short-hairpin RNA (shRNA) sequences against *RPS19* (Figure 6, see R1 and R2) or a control shRNA against Luciferase (Luc) in human K562 cells, and investigated *FLVCR1* gene expression and alternative splicing. RPS19 R1 and R2 shRNA have previously been shown to down-regulate RPS19 in hematopoietic stem cells and specifically disrupt erythroid progenitor cell development.[14] We found that expression of R1 or R2 shRNA in K562 cells reduced *RPS19* gene expression by approximately 39% and 34%, respectively, when compared to *RPS19* gene expression in Luc shRNA-expressing cells (Figure 6A). The reduction in *RPS19* gene expression correlated with a moderate reduction in RPS19 protein expression (Figure 6B, R1 and R2). We next quantified total *FLVCR1* transcript expression using the E1/αE1 primers and the procedures described above. As shown

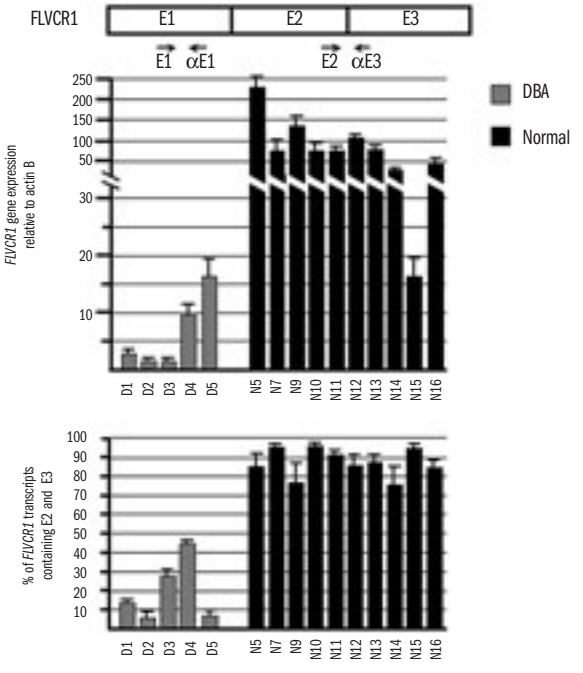

Figure 5. Quantification of normal and alternatively spliced *FLVCR1* transcript expression in Diamond Blackfan anemia and normal immature erythroid cells. Total RNA from CD71^{high} cells isolated from Diamond Blackfan anemia and normal bone marrow was used to generate cDNA, and subsequent real time PCR was carried out using specific exon-specific *FLVCR1* primers (A) The specific E1/αE1 and E2/αE3 primers used in the real-time PCR assays are shown in the inset. Total *FLVCR1* transcript expression, relative to actin B gene expression, is shown for five Diamond Blackfan anemia (striped) and ten normal (black) cell samples. Total *FLVCR1* transcript expression was determined by real-time PCR using the E1/αE1 primers (B) Percent of E2 and E3-containing *FLVCR1* transcripts. E2 and E3-containing *FLVCR1* transcripts were quantified by real-time PCR using E2/αE3 primers and the percentage of transcripts containing E2/E3 calculated relative to total *FLVCR1* transcript expression.

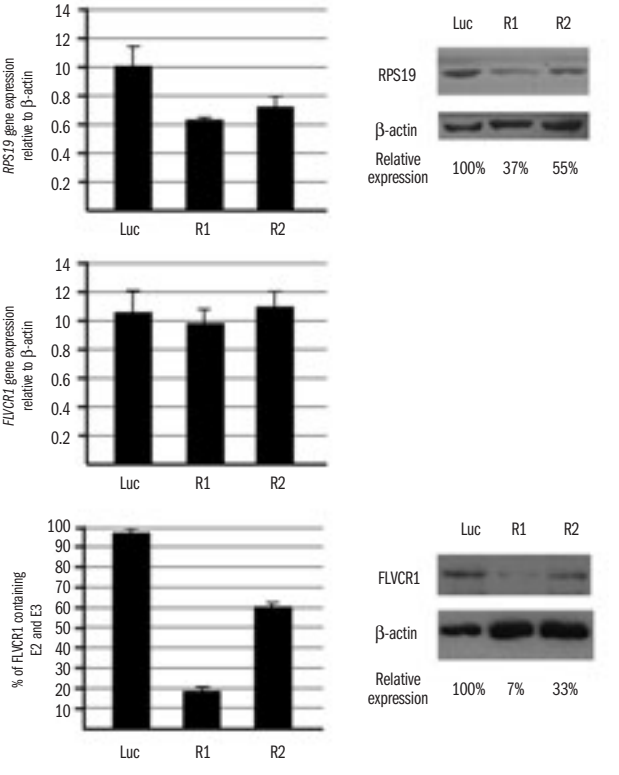

Figure 6. FLVCR1 alternative splicing and protein expression profile in RPS19 down-regulated human K562 cells. RPS19 expression was down-regulated by expression of R1 and R2 RPS19 shRNA. shRNA against the luciferase gene was used as a control. shRNA were introduced into K562 cells by retroviral infection and transduced cells selected using puromycin. *RPS19* and *FLVCR1* gene expression was subsequently determined by real-time PCR using gene-specific primers. Total RPS19 and FLVCR1 protein expression was determined by western blot analysis using specific anti-RPS19 and anti-FLVCR1 monoclonal antibodies. (A) *RPS19* gene expression in R1 and R2 RPS19 shRNA-expressing human K562 cells relative to expression in Luc shRNA-expressing K562 cells. (B) Western blot showing RPS19 protein expression in R1, R2 and Luc shRNA-expressing cells. RPS19 protein expression is shown relative to β-actin expression. (C) Total *FLVCR1* transcript expression in R1 and R2 cells relative to expression in Luc cells. Total *FLVCR1* transcript expression was determined by real-time PCR using the E1/αE1 primers (Figure 5A) (D) Percentage of *FLVCR1* transcripts containing E2 and E3 in R1, R2 and Luc cells relative to total *FLVCR1* transcript expression. (E) Western blot showing total cellular expression of FLVCR1 protein in R1, R2 and Luc cells. FLVCR1 expression is shown relative to β-actin expression.

in Figure 6C, total *FLVCR1* transcript expression in R1 and R2 cells was comparable to expression in Luc cells, suggesting that down-regulation of RPS19 did not disrupt *FLVCR1* gene expression. Interestingly, we found that only 18% and 60% of *FLVCR1* transcripts in R1 and R2 cells, respectively, contained both E2 and E3 when compared to E2/E3-containing *FLVCR1* transcripts in Luc cells (Figure 6D). The reduction in E2/E3-containing *FLVCR1* transcripts in R1 and R2 cells correlated with, respectively, a 93% and 67% down-regulation in total FLVCR1 protein expression (Figure 6E). These findings suggest severe disruption in E2 and E3 in the RPS19-reduced cells and implies enhanced alternative splicing of *FLVCR1* in RPS19 down-regulated cells. Moreover, these findings imply enhanced alternative *FLVCR1* splicing in DBA patients with *RPS19* gene mutations.

Discussion

DBA has been suggested to be caused by a defect in ribosome biogenesis and subsequent defect in translation and protein synthesis but this fails to explain the specificity of the DBA anemia. In this study, we provide evidence that suggests enhanced alternative splicing of *FLVCR1*, and subsequent FLVCR1 protein insufficiency, as an additional contributing factor to the erythropoietic defect observed in DBA. We provide evidence suggesting that FLVCR1 is critical for early erythropoiesis but not myelopoiesis, which recapitulates the hematologic features of DBA. More importantly, our results suggest enhanced alternative splicing of *FLVCR1* transcripts, which disrupts FLVCR1 protein expression and function, in DBA immature erythroid cells negative for *RPS19* gene mutations, and in RPS19-reduced human K562 cells, which we used as a model to represent *RPS19* gene mutated DBA.

Although two previous studies have reported a critical role for FLVCR1 in early erythropoiesis using human K562 cells or *FLVCR1* null mice, our study is the first to show a critical role for FLVCR1 in erythropoiesis using human hematopoietic stem cells, and that a disruption of FLVCR1, as a consequence of FeLV-C Env expression, specifically disrupts early erythropoiesis but not myelopoiesis. These findings provide a more direct correlation with the hematologic features of DBA than did the two previous studies, and raise the possibility of a critical role for FLVCR1 in DBA. Moreover, our observation that FeLV-C Env, and not FeLV-B Env, directly disrupts early erythropoiesis and not myelopoiesis provides more direct evidence that the DBA-related, FeLV-C- induced anemia in domestic cats is caused by FeLV-C Env protein disrupting the feline homolog of FLVCR1.

To further investigate a potential role for FLVCR1 in DBA, we analyzed FLVCR1 sequences expressed in $CD71^{high}$ cells (enriched for immature erythroid cells) isolated from DBA bone marrow samples that were negative for *RPS19* gene mutations, and from normal bone marrow. We found that both DBA and normal samples express alternatively spliced *FLVCR1* transcripts but more importantly our results suggest that alternative splicing of *FLVCR1*, specifically E2 and/or E3 skipping, is significantly enhanced in the DBA cell samples compared to in normal cell samples. The significance of alternatively spliced *FLVCR1* in the DBA samples is further compounded by the dramatic reduction in *FLVCR1* gene expression observed in the DBA samples (Figure 5A). Interestingly, our results suggest, within the limitations of this study, that alternative splicing is specific to *FLVCR1* as we were only able to amplify full-length but not alternatively spliced sequences encoding the FeLV-B receptor Pit1 and the erythropoietin receptor (*data not shown*). However, further detailed investigations are necessary to fully elucidate the specificity of *FLVCR1* alternative splicing in DBA.

We show in this study that the cellular expression, surface localization and receptor function of alternatively spliced $E3^-$ and $E3^-E6^-$ encoded proteins are disrupted. The heme export function of the $E3^-$ and $E3^-E6^-$ encoded proteins was not determined in this study. However, a previous study showed that the corresponding E3 deletion in murine FLVCR1 completely abrogates heme export function[31] suggesting that the $E3^-$ and $E3^-E6^-$ encoded proteins in this study could also have defective heme export function. It is interesting to note that despite the $E3^-$ and $E3^-E6^-$ sequences being in-frame, expression of the respective encoded proteins was severely reduced. It is unclear from this study whether the alternatively spliced transcripts or the encoded proteins are unstable and hence degraded. Our observation that RPS19 down-regulation does not disrupt total *FLVCR1* transcript expression but dramatically enhances alternative splicing would suggest that the alternatively spliced transcripts are stable but that the encoded protein is unstable and hence degraded. This would be consistent with a previous study showing that in-frame alternative splicing disrupts expression of the encoded protein.[44] It is conceivable that alternative splicing may severely disrupt the correct folding of the encoded protein thus making it unstable and hence primed for degradation.[45] The mechanism of how in-frame alternative splicing results in reduced protein expression is fascinating but has yet to be elucidated. The $E2^-$ transcript, although not characterized in this study, is also likely to be non-functional because splicing of E2 creates a premature termination codon (Figure 3B) resulting in the potential expression of a truncated protein that lacks the E3 encoded sequence required for heme export.[31] Moreover, the $E2^-$ transcript could be degraded by the nonsense-mediated decay pathway, which is a quality control mechanism that selectively degrades mRNA containing premature termination codons.[46] These findings suggest that expression of normally spliced *FLVCR1* transcript is substantially reduced in DBA samples as a result of enhanced alternative splicing. We calculated that, on average, there was an approximate 58-fold less normally spliced *FLVCR1* transcript in the DBA samples than in the normal samples. Taken together, our findings suggest a dramatic disruption in FLVCR1 protein expression and function as a consequence of enhanced alternative *FLVCR1* splicing in the DBA samples. Because of the limited availability of sample material, we were not able to assess FLVCR1 protein expression in the DBA or normal cells. However, our cell culture model (Figure 6) showed that a 40-80% enhancement in alternatively

spliced *FLVCR1* down-regulated FLVCR1 protein expression by 67-93%, indicating a severe disruption in FLVCR1 protein expression in the samples from DBA patients.

To investigate alternative splicing of *FLVCR1* in *RPS19* gene mutated DBA, we used RPS19 down-regulated human K562 cells as a model. Interestingly, a moderate down-regulation of *RPS19* gene and protein expression did not disrupt total *FLVCR1* gene expression but significantly enhanced *FLVCR1* alternative splicing, which correlated with a dramatic reduction in total FLVCR1 protein expression. It is unclear from our studies why total *FLVCR1* gene expression is normal in RPS19 down-regulated K562 cells but is down-regulated in samples from DBA patients. It is conceivable that additional factors that specifically regulate *FLVCR1* gene expression are also disrupted in the DBA erythroid cells. However, it is clearly evident from our study that *FLVCR1* gene expression level is not a common factor in DBA, as both samples D5 and N15 had similar total *FLVCR1* gene expression. What is evident from our study is enhanced alternative splicing of *FLVCR1* as seen in all five DBA samples and in the RPS19 down-regulated K562 cells, and that reduced total *FLVCR1* gene expression compounds the contribution of *FLVCR1* alternative splicing in DBA. Moreover, our results show for the first time a potential relationship between a ribosomal protein implicated in DBA and FLVCR1, and raises the possibility of a potential relationship between FLVCR1 and other ribosomal proteins implicated in DBA. It is not clear from this study how a reduction in RPS19 expression enhances *FLVCR1* alternative splicing. It is conceivable that a moderate disruption in RPS19 expression may cause subtle changes in translation efficiency that dysregulates expression of specific cellular factors that regulate splicing of *FLVCR1* transcripts. Alternatively, RPS19 may have extraribosomal functions[47] that control, either directly or indirectly, alternative splicing. RPS19 has been shown to act as a chemotactic factor for monocytes during clearance of apoptotic cells,[48,49] and has also been found to interact with proteasomes and integrins, and splicing factors. Interestingly, RPS19 also interacts with specific serine-arginine rich proteins[50] that have been shown to be involved in regulating alternative splicing of genes,[51] and which have been implicated in human diseases.[52,53] Further detailed investigations are necessary to fully elucidate a potential relationship between ribosomal proteins implicated in DBA and FLVCR1.

In conclusion, based on our findings in this study, we propose enhanced alternative splicing of the *FLVCR1* transcript, specifically skipping of *FLVCR1* E2 and/or E3, and subsequent insufficiency in FLVCR1 protein expression and function, as an additional contributing factor for the erythropoietic defect observed in DBA. How FLVCR1 specifically regulates erythropoiesis remains unclear. Quigley *et al.*[30] and Keel *et al.*[31] have proposed that the heme export function of FLVCR1 regulates intracellular heme levels, which is critical for CFU-E development where FLVCR1 expression is high.[30] The authors proposed that a disruption in FLVCR1 heme export leads to heme toxicity and apoptosis of CFU-E. While further investigations are needed to establish the *heme toxicity* mechanism, it is evident from our study that in DBA there is enhanced alternative splicing of *FLVCR1* transcripts, which disrupts FLVCR1 expression and function that are specifically critical for erythroid progenitor cell development.

Authorship and Disclosures

MAR performed the studies represented in Figures 3, 4 and 5; SPD performed the studies represented in Figure 6; JKB performed the studies represented in Figures 1 and 2; JAK contributed vital new reagents and analytical tools for the studies represented in Figure 2; JED contributed vital new reagents and provided guidance for the studies represented in Figure 2; YD: provided DBA and normal bone marrow samples and contributed to techniques to isolate and characterize CD71 positive cells. The authors reported no potential conflicts of interest.

References

1. Ball SE, McGuckin CP, Jenkins G, Gordon-Smith EC. Diamond-Blackfan anaemia in the U.K.: analysis of 80 cases from a 20-year birth cohort. Br J Haematol 1996;94:645-53.
2. Diamond LK. Congenital hypoplastic anemia: Diamond-Blackfan syndrome. Historical and clinical aspects. Blood Cells 1978;4:209-13.
3. Dianzani I, Garelli E, Ramenghi U. Diamond-Blackfan anemia: a congenital defect in erythropoiesis. Haematologica 1996;81:560-72.
4. Campagnoli MF, Garelli E, Quarello P, Carando A, Varotto S, Nobili B, et al. Molecular basis of Diamond-Blackfan anemia: new findings from the Italian registry and a review of the literature. Haematologica 2004;89:480-9.
5. Dianzani I, Garelli E, Ramenghi U. Diamond-Blackfan anaemia: an overview. Paediatr Drugs 2000;2:345-55.
6. Vlachos A, Federman N, Reyes-Haley C, Abramson J, Lipton JM. Hematopoietic stem cell transplantation for Diamond Blackfan anemia: a report from the Diamond Blackfan Anemia Registry. Bone Marrow Transplant 2001;27:381-6.
7. Wiktor-Jedrzejczak W, Szczylik C, Pojda Z, Siekierzynski M, Kansy J, Klos M, et al. Success of bone marrow transplantation in congenital Diamond-Blackfan anaemia: a case report. Eur J Haematol 1987;38:204-6.
8. Willig TN, Niemeyer CM, Leblanc T, Tiemann C, Robert A, Budde J, et al. Identification of new prognosis factors from the clinical and epidemiologic analysis of a registry of 229 Diamond-Blackfan anemia patients. DBA group of Societe d'Hematologie et d'Immunologie Pediatrique (SHIP), Gesellshaft fur Padiatrische Onkologie und Hamatologie (GPOH), and the European Society for Pediatric Hematology and Immunology (ESPHI). Pediatr Res 1999;46:553-61.
9. Aquino VM, Buchanan GR. Osteogenic sarcoma in a child with transfusion-dependent Diamond-Blackfan anemia. J Pediatr Hematol Oncol 1996;18:230-2.
10. Lipton JM, Federman N, Khabbaze Y, Schwartz CL, Hilliard LM, Clark JI, et al. Osteogenic sarcoma associated with Diamond-Blackfan anemia: a report from the Diamond-Blackfan Anemia Registry. J Pediatr Hematol Oncol 2001;23:39-44.
11. Draptchinskaia N, Gustavsson P, Andersson B, Pettersson M, Willig TN, Dianzani I, et al. The gene encoding ribosomal protein S19 is mutated in Diamond-Blackfan anaemia. Nat Genet 1999;21:169-75.
12. Willig TN, Draptchinskaia N, Dianzani I, Ball S, Niemeyer C, Ramenghi U, et al. Mutations in ribosomal protein S19 gene and Diamond Blackfan anemia: wide variations in phenotypic expression. Blood 1999; 94:4294-306.
13. Flygare J, Aspesi A, Bailey JC, Miyake K, Caffrey JM, Karlsson S, et al. Human RPS19, the gene mutated in Diamond-Blackfan anemia, encodes a ribosomal protein required for the

maturation of 40S ribosomal subunits. Blood 2007;109:980-6.
14. Ebert BL, Lee MM, Pretz JL, Subramanian A, Mak R, Golub TR, et al. An RNA interference model of RPS19 deficiency in Diamond-Blackfan anemia recapitulates defective hematopoiesis and rescue by dexamethasone: identification of dexamethasone-responsive genes by microarray. Blood 2005;105:4620-6.
15. Flygare J, Kiefer T, Miyake K, Utsugisawa T, Hamaguchi I, Da Costa L, et al. Deficiency of ribosomal protein S19 in CD34+ cells generated by siRNA blocks erythroid development and mimics defects seen in Diamond-Blackfan anemia. Blood 2005;105: 4627-34.
16. Hamaguchi I, Ooka A, Brun A, Richter J, Dahl N, Karlsson S. Gene transfer improves erythroid development in ribosomal protein S19-deficient Diamond-Blackfan anemia. Blood 2002;100:2724-31.
17. Matsson H, Davey EJ, Draptchinskaia N, Hamaguchi I, Ooka A, Leveen P, et al. Targeted disruption of the ribosomal protein S19 gene is lethal prior to implantation. Mol Cell Biol 2004;24: 4032-7.
18. Cmejla R, Cmejlova J, Handrkova H, Petrak J, Pospisilova D. Ribosomal protein S17 gene (RPS17) is mutated in Diamond-Blackfan anemia. Hum Mutat 2007;28:1178-82.
19. Gazda HT, Grabowska A, Merida-Long LB, Latawiec E, Schneider HE, Lipton JM, et al. Ribosomal protein S24 gene is mutated in Diamond-Blackfan anemia. Am J Hum Genet 2006;79:1110-8.
20. Flygare J, Karlsson S. Diamond-Blackfan anemia: erythropoiesis lost in translation. Blood 2007;109:3152-4.
21. Jarrett O, Laird HM, Hay D. Determinants of the host range of feline leukemia viruses. J Gen Virol 1973;20: 169-75.
22. Neil JC, Fulton R, Rigby M, Stewart M. Feline leukaemia virus: generation of pathogenic and oncogenic variants. Curr Top Microbiol Immunol 1991;171:67-93.
23. Sarma PS, Log T. Subgroup classification of feline leukemia and sarcoma viruses by viral interference and neutralisation tests. Virology 1973;54: 160-9.
24. Quigley JG, Gazda H, Yang Z, Ball S, Sieff CA, Abkowitz JL. Investigation of a putative role for FLVCR, a cytoplasmic heme exporter, in Diamond-Blackfan anemia. Blood Cells Mol Dis 2005;35:189-92.
25. Abkowitz JL. Retrovirus-induced feline pure red blood cell aplasia: pathogenesis and response to suramin. Blood 1991;77:1442-51.
26. Abkowitz JL, Holly RD, Grant CK. Retrovirus-induced feline pure red cell aplasia. Hematopoietic progenitors are infected with feline leukemia virus and erythroid burst-forming cells are uniquely sensitive to heterologous complement. J Clin Invest 1987;80:1056-63.
27. Quigley JG, Burns CC, Anderson MM, Lynch ED, Sabo KM, Overbaugh J, et al. Cloning of the cellular receptor for feline leukemia virus subgroup C (FeLV-C), a retrovirus that induces red cell aplasia. Blood 2000;95:1093-9.
28. Rigby MA, Rojko JL, Stewart MA, Kociba GJ, Cheney CM, Rezanka LJ, et al. Partial dissociation of subgroup C phenotype and in vivo behaviour in feline leukaemia viruses with chimeric envelope genes. J Gen Virol 1992;73:2839-47.
29. Tailor CS, Willet BJ, Kabat D. A putative cell surface receptor for anemia-inducing subgroup C feline leukemia virus is a member of a transporter superfamily. J Virol 1999;73:6500-5.
30. Quigley JG, Yang Z, Worthington MT, Phillips JD, Sabo KM, Sabath DE, et al. Identification of a human heme exporter that is essential for erythropoiesis. Cell 2004;118:757-66.
31. Keel SB, Doty RT, Yang Z, Quigley JG, Chen J, Knoblaugh S, et al. A heme export protein is required for red blood cell differentiation and iron homeostasis. Science 2008;319:825-8.
32. Dror Y, Freedman MH. Shwachman-Diamond syndrome marrow cells show abnormally increased apoptosis mediated through the Fas pathway. Blood 2001;97:3011-6.
33. Dror Y. Inherited Bone Marrow Failure Syndromes. In: Arececi HS, editor. Pediatric Hematology. Oxford: Blackwell; 2006. p. 30-6.
34. Cosset FL, Takeuchi Y, Battini JL, Weiss RA, Collins MKL. High-titer packaging cells producing recombinant retroviruses resistant to human serum. J Virol 1995;69:7430-6.
35. Tailor CS, Kabat D. Variable regions A and B in the envelope glycoproteins of feline leukemia virus subgroup B and amphotropic murine leukemia virus interact with discrete receptor domains. J Virol 1997;71: 9383-91.
36. Brown J, Fung C, Tailor C. Comprehensive mapping of receptor-functioning domains of feline leukemia virus subgroup C receptor FLVCR1. J Virol 2006;80:1742-51.
37. Pereira DS, Dorrell C, Ito CY, Gan OI, Murdoch B, Rao VN, et al. Retroviral transduction of TLS-ERG initiates a leukemogenic program in normal human hematopoietic cells. Proc Natl Acad Sci USA 1998;95:8239-44.
38. Brojatsch J, Kristal BS, Viglianti GA, Khiroya R, Hoover EA, Mullins JI. Feline leukemia virus subgroup C phenotype evolves through distinct alterations near the N terminus of the envelope surface glycoprotein. Proc Natl Acad Sci USA 1992;89:8457-61.
39. Kavanaugh MP, Miller DG, Zhang W, Law W, Kozak SL, Kabat D, et al. Cell-surface receptors for gibbon ape leukemia virus and amphotropic murine retrovirus are inducible sodium-dependent phosphate symporters. Proc Natl Acad Sci USA 1994; 91:7071-5.
40. Takeuchi Y, Vile RG, Simpson G, O'Hara B, Collins MKL, Weiss RA. Feline leukemia virus subgroup B uses the same cell surface receptor as gibbon ape leukemia virus. J Virol 1992;66:1219-22.
41. O'Hara B, Johann SV, Klinger HP, Blair DG, Rubinson H, Dunn KJ, et al. Characterization of the human gene conferring sensitivity to infection by gibbon ape leukemia virus. Cell Growth Differ 1990;1:119-27.
42. Rogers CE, Bradley MS, Palsson BO, Koller MR. Flow cytometric analysis of human bone marrow perfusion cultures: erythroid development and relationship with burst-forming units-erythroid. Exp Hematol 1996; 24:597-604.
43. Maouche L, Tournamille C, Hattab C, Boffa G, Cartron J, Chretien S. Cloning of the gene encoding the human erythropoietin receptor. Blood 1991;15:2557-63.
44. Calarco JA, Xing Y, Caceres M, Calarco JP, Xiao X, Pan Q, et al. Global analysis of alternative splicing differences between humans and chimpanzees. Genes Dev 2007;21: 2963-75.
45. Tress ML, Martelli PL, Frankish A, Reeves GA, Wesselink JJ, Yeats C, et al. The implications of alternative splicing in the ENCODE protein complement. Proc Natl Acad Sci USA 2007;104:5495-500.
46. Chang YF, Imam JS, Wilkinson MF. The nonsense-mediated decay RNA surveillance pathway. Annu Rev Biochem 2007;76:51-74.
47. Morimoto K, Lin S, Sakamoto K. The functions of RPS19 and their relationship to Diamond-Blackfan anemia: a review. Mol Genet Metab 2007;90: 358-62.
48. Horino K, Nishiura H, Ohsako T, Shibuya Y, Hiraoka T, Kitamura N, et al. A monocyte chemotactic factor, S19 ribosomal protein dimer, in phagocytic clearance of apoptotic cells. Lab Invest 1998;78:603-17.
49. Nishiura H, Shibuya Y, Yamamoto T. S19 ribosomal protein cross-linked dimer causes monocyte-predominant infiltration by means of molecular mimicry to complement C5a. Lab Invest 1998;78:1615-23.
50. Orru S, Aspesi A, Armiraglio M, Caterino M, Loreni F, Ruoppolo M, et al. Analysis of the ribosomal protein S19 interactome. Mol Cell Proteomics 2007;6:382-93.
51. Sanford JR, Ellis J, Caceres JF. Multiple roles of arginine/serine-rich splicing factors in RNA processing. Biochem Soc Trans 2005;33:443-6.
52. Kondo S, Yamamoto N, Murakami T, Okumura M, Mayeda A, Imaizumi K. Tra2 β, SF2/ASF and SRp30c modulate the function of an exonic splicing enhancer in exon 10 of tau pre-mRNA. Genes Cells 2004;9:121-30.
53. Watermann DO, Tang Y, Zur Hausen A, Jager M, Stamm S, Stickeler E. Splicing factor Tra2-beta1 is specifically induced in breast cancer and regulates alternative splicing of the CD44 gene. Cancer Res 2006;66: 4774-80.